

ChemComm

Accepted Manuscript



This is an *Accepted Manuscript*, which has been through the Royal Society of Chemistry peer review process and has been accepted for publication.

Accepted Manuscripts are published online shortly after acceptance, before technical editing, formatting and proof reading. Using this free service, authors can make their results available to the community, in citable form, before we publish the edited article. We will replace this *Accepted Manuscript* with the edited and formatted *Advance Article* as soon as it is available.

You can find more information about *Accepted Manuscripts* in the [Information for Authors](#).

Please note that technical editing may introduce minor changes to the text and/or graphics, which may alter content. The journal's standard [Terms & Conditions](#) and the [Ethical guidelines](#) still apply. In no event shall the Royal Society of Chemistry be held responsible for any errors or omissions in this *Accepted Manuscript* or any consequences arising from the use of any information it contains.

COMMUNICATION

Fluorine-modified bisbenzimidazole derivative as a molecular probe for bimodal and simultaneous detection of DNAs by ^{19}F NMR and fluorescence

Cite this: DOI: 10.1039/x0xx00000x

Received 00th January 2012,
Accepted 00th January 2012Takashi Sakamoto,^{*a} Daisaku Hasegawa^a and Kenzo Fujimoto^{*a,b}

DOI: 10.1039/x0xx00000x

www.rsc.org/

3,5-Bis(trifluoromethyl)benzene modified bisbenzimidazole H 33258 was synthesized as a ^{19}F magnetic resonance-based DNA detection probe. The chemical shift and fluorescence of the probe were significantly changed by the addition of hairpin DNAs having an AATT sequence. The probe enables ^{19}F NMR/fluorescence bimodal detection of the model DNA double strands simultaneously.

The ^{19}F magnetic resonance (MR)-based molecular probe has many potential applications in biological analysis such as imaging of biomolecules *in vivo*, in bio-organs and in crude biological specimens. Because of the high sensitivity of ^{19}F MR signals (approximately 83% of ^1H), and the low background signal from endogenous ^{19}F atoms, the method is expected to be a powerful tool for imaging biomolecules *in vivo*. To date, various ^{19}F MR-based molecular probes that can detect or image biomolecules *in vivo* or in cells have been reported. For example, Higuchi et al. successfully developed a molecular probe for amyloid beta plaque in mouse brains;¹ Mizukami et al. reported a peptide based probe that can detect protease activity in a signal turn-on manner;² Hamachi et al. reported a supramolecular disassembly driven signal turn-on probe that can detect various proteins and enzymes in cells.³ ^{19}F MR-based oligonucleotide probes for detecting nucleic acids have also been developed.⁴ These probes have opened the door to the analysis of endogenous nucleic acids by ^{19}F NMR/MRI; however, there has been no report on probes that can detect nucleic acids in living cells because of the low cell permeability of the oligonucleotide based probe. Therefore, development of a ^{19}F NMR-based nucleic acids detection probe having high cell permeability is required.

As another advantage of ^{19}F NMR, the narrow ^{19}F MR signal is useful to discriminate different molecules or the states of a molecule in a ^{19}F NMR spectrum. This provides simultaneous detection method for various nitrile compounds,⁵ different

ubiquitin chains⁶ and various conformations of DNA.⁷ However, molecular probe that shows different ^{19}F MR signal dependent on the nucleic acids sequence, and that can discriminate nucleic acids having different sequences on a ^{19}F NMR spectra has not been reported.

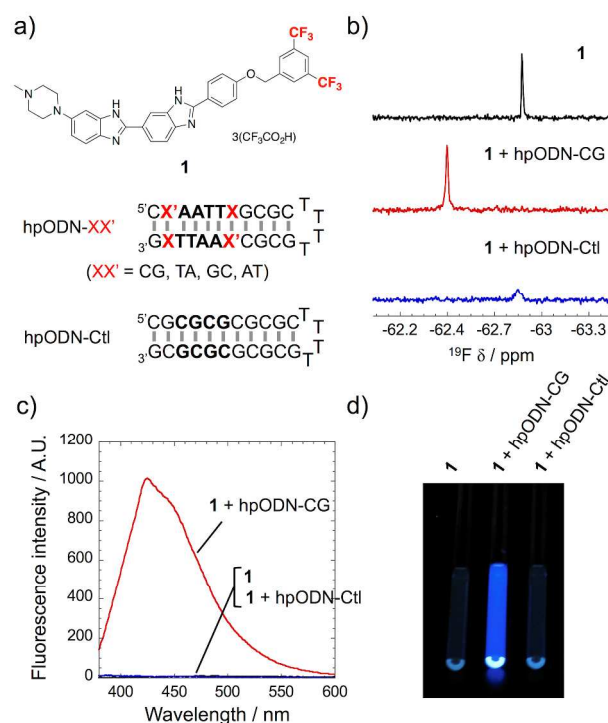


Fig. 1. (a) Structure of fluorine labeled bisbenzimidazole H 33258 (**1**) and the sequences of the ODNs used. (b) ^{19}F NMR, (c) fluorescence spectra and (d) fluorescence image of **1** in the presence of hpODN-CG or hpODN-Ctl. [**1**] = [hpODN] = 10 μM in 50 mM Tris-HCl (pH 7.6) containing 100 mM NaCl and 10% (v/v) D_2O . Measurements were performed at 27°C. Fluorescence image was obtained under 365 nm irradiation with a transilluminator using the samples in NMR tubes after the ^{19}F NMR measurements.

In this study, to obtain a ^{19}F MR-based DNA detection probe having cell permeability and the ability for discriminating sequences around the binding site of the probe, we designed a novel probe molecule consisting of bisbenzimidazole H 33258 and 3,5-bis(trifluoromethyl)benzene as a DNA recognition moiety and a ^{19}F source, respectively (Fig. 1a). As the bisbenzimidazole H 33258, *i.e.* Hoechst 33258, is a general fluorescent probe for DNA imaging in living cells and as a designed probe (compound **1**) has the positive net charge, **1** may have high cell permeability similar to bisbenzimidazole H 33258. Furthermore, fluorescence and ^{19}F NMR bimodal detection of DNA is expected using **1**. Synthesis of **1** was performed using commercially available bisbenzimidazole H 33258 and 3,5-bis(trifluoromethyl)benzylbromide, and **1** was successfully purified by high performance liquid chromatography (See ESI⁸).

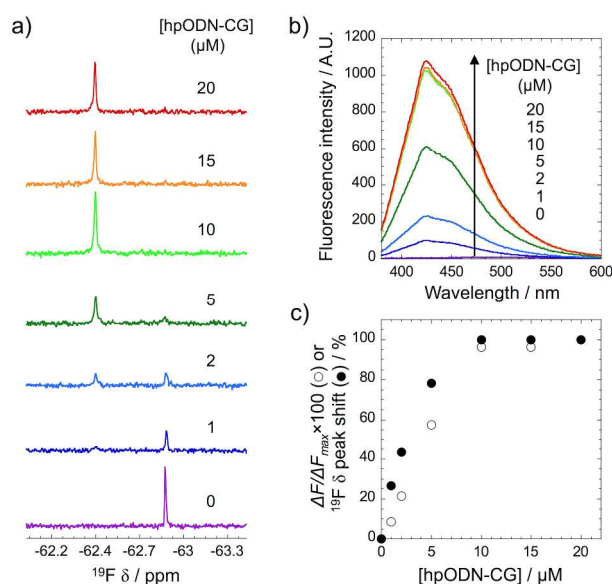


Fig. 2. (a) ^{19}F NMR and (b) fluorescence spectra of **1** in the presence of various concentrations of hpODN-CG. (c) Titration curves derived from the ratio of the peak shift in ^{19}F NMR and fluorescence enhancement at 460 nm. [**1**] = 10 μM in 50 mM Tris-HCl (pH 7.6) containing 100 mM NaCl and 10% (v/v) D_2O . Measurements were performed at 27°C.

First, to examine the ^{19}F MR chemical shift change through the binding with hairpin oligodeoxyribonucleotide (hpODN), ^{19}F NMR of **1** was measured in the presence of hpODN-CG (Fig. 1a) having an AATT sequence, which is the reported binding site of bisbenzimidazole H 33258,⁸ at the stem region. As shown in Fig. 1b, the ^{19}F MR chemical shift of **1** (−62.89 ppm) was clearly shifted to a lower magnetic field (−62.44 ppm) by the addition of hpODN-CG. The change in the chemical shift of **1** was not observed in the presence of hpODN-Ctl, which has a GGCC sequence instead of AATT in hpODN-CG, indicating that **1** bound to double stranded DNA with AATT selective interaction, which is reported in the case of unmodified bisbenzimidazole H 33258.⁸ The shifted peak was reverted by the addition of unmodified bisbenzimidazole H 33258 (Fig. S1), suggesting that **1** bound the same binding site of unmodified

bisbenzimidazole H 33258. Peak broadening was observed in the case of the addition of hpODN-Ctl, suggesting that **1** interacts non-specifically to hpODN-Ctl with a high chemical exchange rate. The fluorescence spectra of the same samples as ^{19}F NMR experiments are shown in Fig. 1c. The fluorescence of **1** was dramatically enhanced by the addition of hpODN-CG, although the enhancement was not observed in the case of hpODN-Ctl. Together with the results of the ^{19}F NMR experiment, it is strongly suggested that **1** can detect double-stranded DNA having an AATT sequence with fluorescence and ^{19}F MR bimodality.

As the ^{19}F MR peak shift and the fluorescence enhancement of **1** occurred in a hpODN-CG concentration dependent manner (Fig. 2a,b), the quantitative detection of target double-stranded DNA might be possible particularly in the case of ^{19}F NMR ratiometric detection. The titration curves of **1** versus hpODN-CG derived from ^{19}F NMR and fluorescence spectra are shown in Fig. 2c. The fluorescence was linearly increased by the addition of hpODN-CG and the change was saturated with the addition of an equimolar amount of hpODN-CG, suggesting that **1** and hpODN-CG form 1:1 complex the same as the case of unmodified bisbenzimidazole H 33258.⁸ Contrary to the case of fluorescence enhancement, the yield of the ^{19}F NMR peak shift was higher than the molar equivalency of added hpODN. The higher yield appears to be due to the broadening of the initial peak (−62.89 ppm) induced by nonspecific interaction as discussed above.

Table 1. K_D of **1** and bisbenzimidazole H 33258 toward various hpODNs

	$K_D / \times 10^9 \text{ M}^a$	
	1	Bis-benzimidazole H 33258
hpODN-CG	1.6 ± 0.16	1.9 ± 0.06
hpODN-TA	0.2 ± 0.04	0.2 ± 0.08
hpODN-GC	3.4 ± 0.17	3.4 ± 0.11
hpODN-AT	2.3 ± 0.16	1.4 ± 0.09
hpODN-Ctl	n.d. ^b	n.d. ^b

^aValues of K_D were determined by fluorescence titration analysis with nonlinear least-squares curve-fitting (Fig. S2 and Fig. S3). ^bThis value of K_D cannot be determined because the small change in fluorescence intensity occurred after the addition of hpODN-Ctl.

The binding affinity of **1** to various hpODNs was evaluated by fluorescence titration experiments (Fig. S2 and S3). As shown in Table 1, in all cases, dissociation constants (K_D) of **1** were comparable to that of unmodified bisbenzimidazole H 33258, suggesting that the 3,5-bis(trifluoromethyl)benzyl group scarcely affected the interaction between the bisbenzimidazole group and the minor groove in the AATT region of double-stranded DNA.

To evaluate the cell permeability of **1**, HeLa cells were treated with a solution of **1** or bisbenzimidazole H 33258, and then directly observed under a fluorescence microscope. As shown in Fig. 3, bright fluorescence spots were observed in cells in both cases. The fluorescence intensity of the spots in the case of **1** was higher than that in the case of bisbenzimidazole H 33258. This result suggests that the cell permeability of **1** is comparable or greater than that of bisbenzimidazole H 33258. As bisbenzimidazole H

33342, which has a methoxy group instead of a hydroxy group of bisbenzimidazole H 33258, and which has a higher net positive charge than bisbenzimidazole H 33258, has higher cell permeability compared to bisbenzimidazole H 33258,⁹ the enhanced cell permeability of **1** might be caused by the increased net positive charge of **1**.

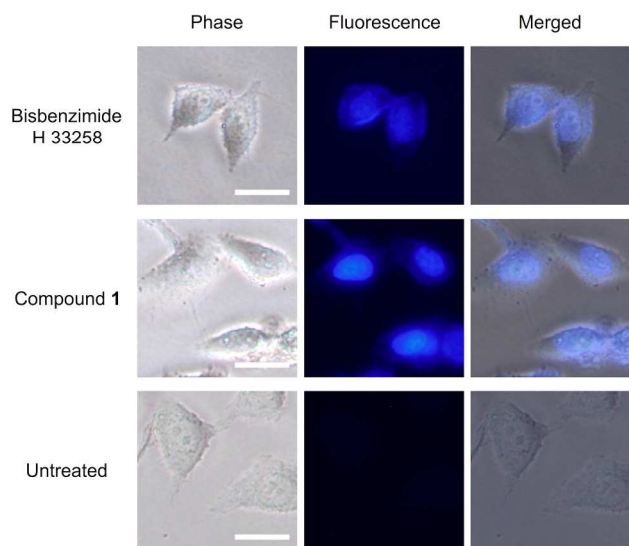


Fig. 3. Fluorescence microscopic analysis of the cell permeability of **1**. HeLa cells plated on glass-bottom dishes were treated with bisbenzimidazole H 33258 (10 μ M) or **1** (10 μ M) in FluoroBrite™ DMEM (37°C, 10 min), and then directly observed by a fluorescence microscope. Scale bar: 25 μ m.

Finally, we measured the ^{19}F NMR spectra of **1** in the presence of various hpODNs. As shown in Fig. 4a, the chemical shift on the ^{19}F NMR spectra differed depending on the base pairs neighboring AATT binding site of bisbenzimidazole moiety, suggesting that the environment, such as the local dielectric constant, around the CF_3 group on **1** differed quite markedly among the four base pairs. The two peaks observed in the case of hpODN-TA, GC and AT indicate that there are two different binding modes between **1** and these hpODNs. As the stem regions around the AATT binding sites have palindromic sequence, **1** can bind in two different directions; 3,5-bis(trifluoromethyl)benzene moiety possessed at the blunt end side or at the T4 loop side. The difference in the environment between these two sides might affect the chemical shift of **1** bound to these hpODNs. Indeed, the ^{19}F NMR spectrum of **1** bound with hpODN having a longer stem region, which has an additional 3 base pairs at the blunt end of hpODN-TA, gave a single peak at -62.36 ppm (Fig. S4), suggesting that the relatively flexible structure of the blunt end affected the chemical shift of **1** bound in the direction that the bis(trifluoromethyl)benzene moiety possessed at the blunt end side of these hpODNs. As the sequence of double-stranded DNA around AATT can be determined from the chemical shift of **1** on a ^{19}F NMR spectrum, sequences of the double-stranded DNA mixture in a solution might be analyzed on a ^{19}F NMR spectrum using **1**. Indeed, the ^{19}F NMR spectrum of the solution including various hpODNs shows various peaks that

are identical to the MR signal from **1** bound to each of the hpODNs (Fig. 4b). With further development, this type of probe could become useful for analyzing DNA in living cells, and also for simultaneous detection of DNAs having different sequences on a ^{19}F NMR spectrum.

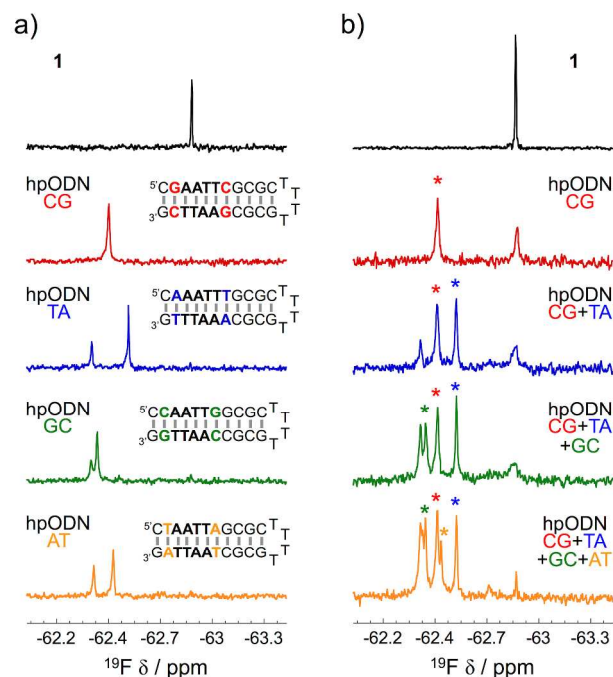


Fig. 4. ^{19}F NMR spectra of **1** in the presence of various hairpin ODNs. (a) 1:1 mixture of **1** and hairpin ODNs having different sequences. [**1**] = [hpODN] = 10 μ M in 50 mM Tris-HCl (pH 7.6) containing 100 mM NaCl and 10% (v/v) D_2O . (b) In the presence of hairpin ODN mixture. [**1**] = 25 μ M, [hpODN] = 5 μ M each in 50 mM Tris-HCl (pH 7.6) containing 100 mM NaCl and 10% (v/v) D_2O . Measurements were performed at 27°C.

Conclusions

In conclusion, the ^{19}F NMR/fluorescence bimodal probe for DNA detection was successfully developed using the bisbenzimidazole skeleton as a double-stranded DNA recognizing motif. Surprisingly, the probe can discriminate the sequence neighbouring AATT binding site by the ^{19}F MR chemical shift. This unique characteristic of the probe enables simultaneous detection of double-stranded DNAs having different sequences on a ^{19}F NMR spectrum, and provides a novel concept for designing the molecular probe for DNA detection and imaging.

This study was partly supported by the Grant-in-Aid for Young Scientists (B) (T.S), Scientific Research on Innovative Areas (Molecular Robotics) (T.S.) and the Grant-in-Aid for Scientific Research (B) (K.F.) of The Ministry of Education, Science, Sports and Culture of Japan.

Notes and references

^a School of Materials Science, Japan Advanced Institute of Science and Technology, 1-1 Asahi-dai, Nomi, Ishikawa 923-1292, Japan

^b Research Center for Bio-Architecture, Japan Advanced Institute of Science and Technology, 1-1 Asahi-dai, Nomi, Ishikawa 923-1292, Japan
Electronic Supplementary Information (ESI) available: Fig. S1–S4 and experimental details. See DOI: 10.1039/c000000x/

- 1 M. Higuchi, N. Iwata, Y. Matsuba, K. Sato, K. Sasamoto, and T. C. Saïdo, *Nat. Neurosci.*, 2005, **8**, 527.
- 2 S. Mizukami, R. Takikawa, F. Sugihara, Y. Hori, H. Tochio, M. Wälchli, M. Shirakawa and K. Kikuchi, *J. Am. Chem. Soc.*, 2008, **130**, 794.
- 3 Y. Takaoka, T. Sakamoto, S. Tsukiji, M. Narazaki, T. Matsuda, H. Tochio, M. Shirakawa and I. Hamachi, *Nat. Chem.*, 2009, **1**, 557; Y. Takaoka, K. Kiminami, K. Mizusawa, K. Matsuo, M. Narazaki, T. Matsuda and I. Hamachi, *J. Am. Chem. Soc.*, 2011, **133**, 11725; K. Matsuo, R. Kamada, K. Mizusawa, H. Imai, Y. Takayama, M. Narazaki, T. Matsuda, Y. Takaoka, and I. Hamachi, *Chem. Eur. J.*, 2013, **19**, 12875.
- 4 T. Sakamoto, Y. Shimizu, J. Sasaki, H. Hayakawa and K. Fujimoto, *Bioorg. Med. Chem. Lett.*, 2011, **21**, 303; A. Kieger, M. J. Wiester, D. Procissi, T. B. Parrish, C. A. Mirkin and C. Shad Thaxton, *Small*, 2011, **7**, 1977; J. Riedl, R. Pohl, L. Rulíšek and M. Hocek, *J. Org. Chem.*, 2012, **77**, 1026.
- 5 Y. Zhao, G. Markopoulos and T. M. Swager, *J. Am. Chem. Soc.*, 2014, **136**, 10683.
- 6 S. S. Shekhawat, G. H. Pham, J. Prabhakaran and E. R. Strieter, *ACS Chem. Biol.*, 2014, **9**, 2229.
- 7 R. Mounné, M. Pasco, E. Prost, T. Lecourt, L. Micouin and C. Tisné, *J. Am. Chem. Soc.*, 2010, **132**, 13111; T. Sakamoto, H. Hayakawa and K. Fujimoto, *Chem. Lett.*, 2011, **40**, 720; K. Tanabe, T. Tsuda, T. Ito and S. Nishimoto, *Chem. Eur. J.*, 2013, **19**, 15133; A. Kiviniemi, M. Murtola, P. Ingman and P. Virta, *J. Org. Chem.*, 2013, **78**, 5153; L. Granqvist and P. Virta, *J. Org. Chem.*, 2014, **79**, 3529.
- 8 F. G. Loontjens, P. Regenfuss, A. Zechel, S. L. Dumortier and R. M. Clegg, *Biochemistry*, 1990, **29**, 9029; S. Y. Breusegem, R. M. Clegg and F. G. Loontjens, *J. Mol. Biol.*, 2002, **315**, 1049.
- 9 D. J. Arndt-Jovin and T. M. Jovin, *Methods Cell Biol.*, 1989, **30**, 417.